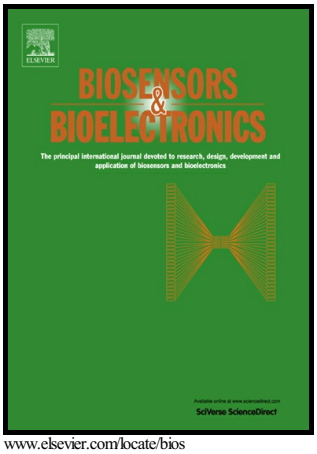

www.elsevier.com/locate/bios

Printable QR code paper microfluidic colorimetric assay for screening volatile biomarkers

Alison Burklund, Harrison K. Saturley-Hall, Flavio A. Franchina, Jane E. Hill, John X.J. Zhang

PII: S0956-5663(18)30980-1
DOI: https://doi.org/10.1016/j.bios.2018.12.026
Reference: BIOS10993

To appear in: *Biosensors and Bioelectronic*

Cite this article as: Alison Burklund, Harrison K. Saturley-Hall, Flavio A. Franchina, Jane E. Hill and John X.J. Zhang, Printable QR code paper microfluidic colorimetric assay for screening volatile biomarkers, *Biosensors and Bioelectronic,* https://doi.org/10.1016/j.bios.2018.12.026

Printable QR code paper microfluidic colorimetric assay for screening volatile biomarkers

Alison Burklund, Harrison K. Saturley-Hall, Flavio A. Franchina, Jane E. Hill, John X.J. Zhang*

Thayer School of Engineering, Dartmouth College, Hanover, NH 03755, USA

*Corresponding author: **Mailing address:** Thayer School of Engineering at Dartmouth, 14 Engineering Drive, Hanover, NH, 03755, USA. **E-mail:** john.zhang@dartmouth.edu.

Abstract

We present a QR code paper microfluidic colorimetric assay that can exploit the hardware and software on mobile devices, and circumvent sample preparation by directly targeting volatile biomarkers. Our platform is a printable microarray of well-defined reaction regions, which outputs an instant diagnosis by directing the user to a URL containing their test result, while simultaneously storing epidemiological data for remote access and bioinformatics. To assist in the rapid identification of *Escherichia coli* in bloodstream infections, we employed an existing colorimetric reagent (*p*-dimethylaminocinnamaldehyde) and adapted its use to detect volatile indole, a biomarker produced by *E. coli*. Our assay was able to quantitatively detect indole in the headspace of *E. coli* culture after 12 h of growth (27.0 ± 3.1 ppm), assisting in species-level identification hours earlier than existing methods. Results were confirmed with headspace solid-phase microextraction (HS-SPME) two-dimensional gas chromatography time-of-flight mass spectrometry (GC×GC-ToFMS), which estimated indole concentration in *E. coli* culture to average 32.3 ± 5.2 ppm after 12 h of growth. This QR paper microfluidic platform represents a novel development in both telemedicine and diagnostics using volatile biomarkers. We envision

that our QR code platform can be extended to other colorimetric assays for real-time diagnostics in low-resource environments.

Keywords

Sepsis; Paper Microfluidics; Volatile Organic Compounds; Mobile Health; Gas Chromatography - Mass Spectrometry

Introduction

There is a need for effective, inexpensive, rapid diagnostics for infectious diseases, especially in low-resource settings [1]. Colorimetric assays are a popular tool for identifying the presence of target molecules and biomarkers associated with both infectious and chronic disease [2-6]. Given that these assays generally require large sample and reagent volumes, microfluidic systems have been pursued as a viable alternative to traditional, macro-scale colorimetric reaction platforms [7-9]. Paper has emerged as an attractive alternative to pressure-driven microfluidic platforms due to its low-cost [10], ease of fabrication [10], and its ability to autonomously drive fluid flow with its imbedded capillary pores [11, 12]. Here, we have designed a paper microfluidic device that can rapidly detect indole-producing *Escherichia coli* (*E. coli*) using a system that bypasses traditional sample preparation steps and utilizes an embedded QR code [13, 14].

Our device leverages existing sensor packages and network connectivity on mobile platforms, in order to eliminate the need for additional external software and hardware [15-17]. Specifically, we have designed an error-correctable QR code-based system to generate two barcodes, each of which contains a set of shared locations to carry out 30 redundant colorimetric assays per device. This redundancy enables quality control through error-correction. In other words, if some locations within the system are defective or suffer from fluid handling errors, the overall

integrity of the test is maintained. When the device is exposed to the target biomarker, assay regions exhibit a concentration-dependent luminance shift. If the color change is above a specified intensity, the reader application will direct the user to the "positive result" URL (child URL); if not, the reader will direct the user to the "negative result" URL (parent URL). Results of the test and other metadata can be stored at these secured URLs for clinical as well as epidemiological use. An overview of assay functionality is shown in **Figure 1**.

Sample preparation requirements are typically a significant barrier to the translation of diagnostic systems into the clinic, especially systems that utilize microfluidic platforms [18]. Currently, numerous colorimetric assays are employed in clinical microbiology laboratories to identify disease-causing organisms [19, 20]. That said, these assays often require at least 24 hours to 1) isolate the pathogenic organism from the patient specimen [19-21], and/or 2) culture the patient specimen onto specialized colorimetric growth media to identify the presence of a target molecule, enzyme, or metabolic product [22].

To minimize sample preparation, the proposed assay targets the detection of volatile indole, a degradation production of tryptophan [23]. Indole tests have been employed as far back as 1889 as a means to differentiate bacterial species belonging to the Enterobacteriaceae family [24].The most sensitive colorimetric reagent used to detect indole is 3-[4-(Dimethylamino)phenyl]prop-2-enal, commonly known as *p*-dimethylaminocinnamaldehyde (DMACA) [25, 26]. With greater than 99% sensitivity to indole, DMACA surpasses the analytical performance other compounds used to identify indole, such as Kovacs indole reagent, *p*-dimethylaminobenzaldehyde (DMABA), and Ehrlich indole reagent [26]. Current use of the DMACA assay (K853009) requires that *E. coli* first be isolated from the biological sample, generally requiring an overnight culture step. Following this, the isolated colony is physically smeared onto filter paper that is

saturated with the reagent [27]. In this work, we have taken this existing colorimetric reagent and adapted its use methodology to detect indole in the gas-phase, effectivity eliminating the previously required time-intensive isolation step.

The diagnosis of bloodstream infections (sepsis) represents one application for the proposed assay. *E. coli* accounts for 16% of all bloodstream infections in the United States [28]. Further, indole is produced by 98% of *E. coli* strains, and is not produced by the majority of other highly prevalent gram-negative sepsis-causing organisms (e.g. *Acinetobacter* spp., *Enterobacter* spp., *Pseudomonas* spp., *Klebsiella pneumoniae*) [20, 28, 29]. In order to diagnose sepsis, a blood culture is first required to affirm the presence of a pathogen in the bloodstream. The median time to blood culture positivity in patients with *E. coli* bacteremia is approximately twelve hours [30]. Following blood culture positivity, a variety of molecular methods and traditional culture based methods are used to identify the sepsis-causing organism(s), which can take anywhere between 2 to 72 additional hours [31, 32]. With accurate organism identification at an earlier time point (i.e. at the time of culture positivity), clinicians are able to more rapidly narrow antibiotic therapy, effectively lowering health care costs [33] and decreasing patient mortality rates [34].

We report on a QR paper microfluidic colorimetric assay used to detect indole in the headspace of three strains of *E. coli* in liquid media. Our results suggest that this assay can be quantitative, given the observed linear relationship between indole concentration and mean gray value intensity of the assay regions. Further, our assay was able to detect indole in three strains of *E. coli* after twelve hours of growth, with the dissolved indole concentration calculated to equal 27.0 ± 3.1 ppm. As a reference method, headspace solid-phase microextraction (HS-SPME) two-dimensional gas chromatography time-of-flight mass spectrometry (GC×GC-ToFMS) was carried out on paired samples to allow for both quantitative analysis and evaluation of device

performance. The proposed system holistically integrates an inexpensive platform, a methodological redesign of an existing colorimetric assay, and a mobile readout infrastructure.

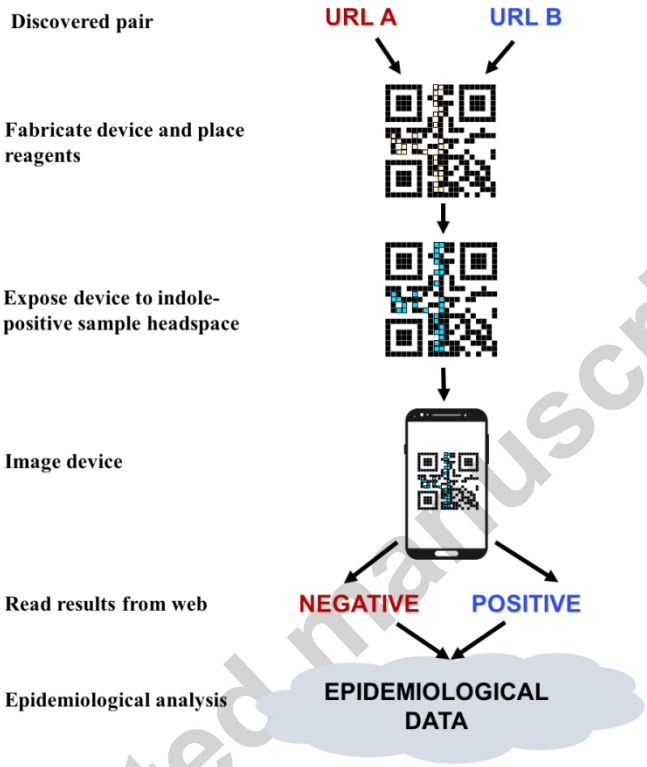

Figure 1. Overview of QR code paper microfluidic colorimetric assay design**.** The fabricated paper device contains an imbedded QR code. The regent is placed in the 30 defined assay regions on the device (as shown in the QR code as blue dots). The device is then exposed to the headspace of the sample of interest to detect volatile biomarkers. The device is imaged, and results are sent to the appropriate URL. The data can be accessed remotely and/or used for broad epidemiological studies.

Methods

Software. The software utilized for device construction was based on Python44, PyQRCode 45, and LATEX 46. The software required to read the device output is ZXing 47. No pre-processing of the captured images is required, as QR code reading applications exist on all mobile and desktop platforms**.**

Algorithm. First, a universal resource locator (URL) was selected to function as the trunk to search for parent-child pairs. A variable region of a fixed number of characters was appended to the end of this URL to define the search space of possible parent and child URLs. Next, a QR code version, error correction level, and character encoding was selected for the total length of the trunk and variable region. A binary array to the QR code specification was then constructed with a length *d*, which contains the encoding information, the data length, the root URL, a zeroed-out variable region, *v*, of length *k*, and with any additional filler bits as specified. Next, the error correcting code (ECC) bits, *e*, were calculated for this array and appended, resulting in an array of length $L = d + e$. We denoted this value as *ROOT*. Given the *k* array positions (*v*1...*k*) in *ROOT* associated with the variable region, *k* binary arrays of length *d* were constructed such that in each array only the *v*1...*k* bit is set to 1. The ECC bits were generated for and appended to each of the *k* arrays, respectively. These *k* arrays of length *L* were denoted as BASIS1...*k*. Finally, one of the set of $MASK_{0...7}$ was chosen, and a binary array of length *L* was constructed, with the bits set according to the equation for the mask for each bit's final position in the QR code. This step violates the QR code specification as the mask is to be chosen to minimize similarity of the data region to the finder patterns, however there is no structural limitation to prevent selection of a specific mask. The results of these steps are structured arrays as shown in **Supplementary Figure S1**. With this separation of elements, we can reduce the scale of the problem of pair regeneration to a search for pairs of sets of *BASIS* vectors in a space that is $O(2^{2k})$ in size instead of $O(2^{2d})$. A naïve approach was developed to search this space and to find pairs of QR codes that are devoid of bit placement errors such that the two QR codes differ only in that a subset of the zero-valued bits in the parent code are one-valued in the child code. This subset of bits composes the set of defined colorimetric assay regions. A positive reaction,

resulting in a colorimetric shift, effectively changes the output value of the barcode. Pseudocode for the algorithm described above is shown **in Supplementary Figure S2**. A schematic overview of the basis structure components and the pair-search algorithm is shown in **Supplementary Figure S3**.

Device Fabrication. The paper based microfluidic devices were fabricated using the process shown **Figure 2A**. First, the design was printed using a Xerox ColorQube 8580 digital wax printer (Xerox Corporation, Norwalk, CT, USA) on Whatman® chromatography grade 1 filter paper (Sigma-Aldrich, St. Louis, MO, USA). Device size specifications are detailed in **Supplementary Figure S4.** Next, the devices were heated at 120^{o}C for 2 min to melt the wax, forming vertical hydrophobic barriers on the hydrophilic paper substrate. A schematic of the printed device functionality is shown in **Figure 2B**. Immediately prior to the time of exposure to the sample headspace, 0.5 µl of Indole DMACA Spot Reagent (Hardy Diagnostics, Santa Maria, CA, USA) was pipetted into each of the 30 defined assay regions on the device. The device was then adhered to the lid of a standard 10 cm disposable petri dish. Device stability was confirmed for up to 45 min post-sample exposure. Long-term device stability was not characterized in this work.

Culture Conditions and Sample Preparation. Three *E. coli* strains were evaluated to assess average indole production levels in *E. coli*: 1) *E. coli* K12 (clinical isolate), 2) *E. coli* ATCC 25922 (reference isolate), and 3) *E. coli* 43890 (reference isolate). All three strains were pre-cultured aerobically overnight (37^{o}C, 200 rpm) in 5 mL Tryptic Soy Broth (TSB) (Becton Dickinson, Franklin Lakes, NJ, United States). Following pre-culture, approximately 3600CFU

were inoculated into 90 mL of fresh TSB (40 CFU/mL), and incubated under identical conditions (37^{o}C, 200 rpm) in 500 mL Erlenmeyer flask. Four identical flasks were prepared for each *E. coli* strain, enabling sampling at 3 h, 6 h, 9 h, and 12 h. At each respective time point, cultures were transferred to 50 mL conical flasks (x3), submerged on ice to quench cellular metabolism, and centrifuged (12,100 × *g*, 25^{o}C, 15 min). Following centrifugation, 20 mL of culture supernatant was transferred to a standard 10 cm disposable petri dish, and the paper device was exposed to the headspace of the sample for 10 min (**Figure 2C**) at 25^{o}C. *Pseudomonas aeruginosa* ATCC 25922 samples were identically prepared. Three technical replicates, using three unique devices, were evaluated for each bacterial strain at each time point.

In parallel, 4 mL of *E. coli* culture supernatant was transferred to a 20 mL air-tight glass headspace vial, sealed with a Silicone/PTFE screw cap (Sigma-Aldrich, St. Louis, MO, USA), and stored at -20^{o}C until analysis. These samples were analyzed within one month of storage. Three technical replicates were prepared for each unique sample. Sterile TSB controls were identically prepared and analyzed at each time point in triplicate.

Indole Standard Preparation.

An indole analytical standard was purchased from Sigma-Aldrich (St. Louis, MO, USA). Indole standards were prepared using 50 mL volumetric flasks by dissolving the solid indole standard into sterile TSB. The following concentrations were prepared to assess the limit of detection of the paper device: 1, 10, 20, 30, 40, and 50 ppm. Identical to the process described above, a 20 mL sample was transferred to a standard 10 cm disposable petri dish, and the paper device was exposed to the headspace of the sample for 10 min at 25^{o}C (**Figure 2C**). Three technical replicates, using three unique devices, were evaluated for each concentration value. For the HS-

SPME GCxGC-ToFMS analysis [35] the following concentrations were used to construct a calibration curve: 2, 5, 10, 25, 33, and 40 ppm. Identical to the process described above, a 4 mL sample was transferred to a 20 mL air-tight glass headspace vial and sealed with a Silicone/PTFE screw cap (Sigma-Aldrich, St. Louis, MO, USA) and stored at -20^{o}C until analysis. These samples were analyzed within one month of storage. Three technical replicates were prepared for each concentration value. Sterile TSB controls were identically prepared and analyzed in triplicate.

Image Processing.

Device exposure to indole-positive samples resulted in varying levels of colorimetric shift and intensity on the device. In order to quantify color intensity, devices were scanned as 1200 dpi PDFs using a HP Photosmart C3180 printer (Hewlett Packard, Palo Alto, CA, USA) immediately following the 10 min exposure time. Files were then converted to 150pixel/inch JPEG files, and imported into *ImageJ* image processing software (National Institute of Health, Rockville, MD, USA). Within *ImageJ*, mean gray intensity values were automatically calculated as a function manually selected area regions. Given that there are 30 distinct reaction areas per device, 30 intensity values per device could be obtained. Mean gray intensity values were obtained from the 8-bit RGB image by employing the following formula: V=(R+G+B)/3, where V is the mean gray intensity value. Note that the methodology described above allows for more detailed downstream biosensor analytics and characterization, but is different from ZXing, the methodology employed by the QR reader application [36].

Analytical Methods and Instrumentation.

Indole concentration was further quantified using headspace solid-phase microextraction (HS-SPME) for extraction, and a comprehensive two-dimensional gas chromatography time-of-flight mass spectrometry system (GC×GC-ToFMS) for separation and detection. The latter consisted of a LECO® Pegasus 4D GC×GC-ToFMS (LECO® Corp., St. Joseph, MI, United States) equipped with a rail autosampler (MPS, Gerstel® Inc., Linthcum Heights, MD, United States), gas chromatography (GC) columns produced by Restek® (Bellefonte, PA, United States), and SPME fibers manufactured by Supelco® (Bellefonte, PA, United States) [37]. A comprehensive description of instrumental parameters is presented in **Supplementary Table S5**.

Data Availability.

The datasets generated during and analyzed during the current study are available from the corresponding author on reasonable request.

Results

Device fabrication, assay functionality, and experimental setup.

The QR code paper microfluidic colorimetric assay was fabricated using the process outlined in **Figure 2A**. First, the device was printed using a wax printer. Next, the device was then heated at 120^{o}C for 2 min to melt wax and create defined hydrophilic and hydrophobic regions in the paper. Finally, 5 μl of DMACA reagent was manually pipetted into the 30 hydrophilic assay regions. Device fabrication required less than 5 min per device, with materials costs totaling less than $0.50 per device. Following device fabrication, the device was exposed to the headspace of a suspected indole-positive sample. The appearance of a blue-green compound indicated the presence of indole in the sample (**Figure 2A & 2B**). In order to assess the limit of detection and clinical relevance of this platform, experiments were performed using indole standard solutions

along with three indole-producing *E. coli* strains. The assay was evaluated at room temperature (25^{o} C) and 35-40% humidity, making the results repeatable in any temperature controlled laboratory environment.

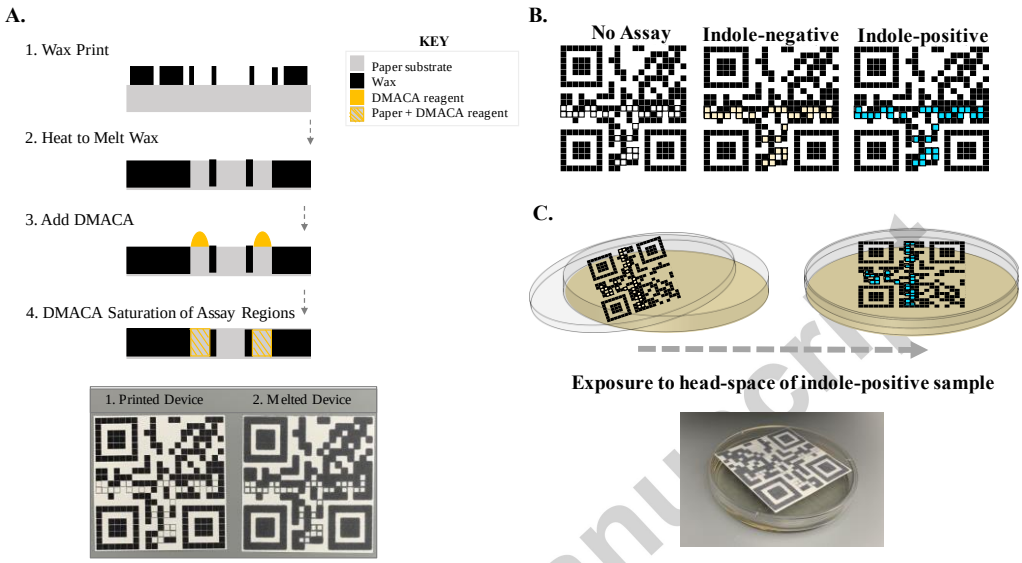

Figure 2. (A) Cross-sectional view of device fabrication and top-down images of fabricated device (steps 1-2). 1) Device is printed using a wax printer. 2) Device is heated to melt wax. 3) DMACA reagent is added to 30 assay regions. 4) DMACA reagent saturates the 30 assay regions. The device is now ready for exposure to the headspace of the sample. **(B)** Schematic of device at different stages of construction to illustrate theory of device functionality. The result is read as positive if assay regions turn blue-green when the device is exposed to a sample with detectable volatile indole concentration. **(C)** Schematic and image of experimental setup for device exposure to sample headspace. A 20 mL sample is added to a standard disposable Petri dish. The device is adhered to the lid of the Petri dish and placed over the sample for 10 min at 25^{o}C.

Assay exposure to indole standard solution headspace.

In order to assess dynamic range of the assay, devices were exposed to the headspace of indole analytical standard solutions with known concentrations, ranging from 1 to 50 ppm. Prior to any data analysis and image processing, the first evident color change was observed at 10 ppm (**Figure 3A**). By employing some basic image processing tools (ImageJ), the mean gray value intensity for each assay region on the device was calculated. Since each device contains 30 unique assay regions, 30 data points were obtained per device. By averaging these 30 intensity

values, the mean color intensity of the device when exposed to a 1 ppm standard solution was found to be statistically greater than color intensity observed at 0 ppm (**Figure 3B**). Depending on the specific application of this assay, the increased detection sensitivity obtained by employing basic imaging processing tools on a mobile platform could be of value. Additionally, the results from this analysis indicate that the mean color intensity correlates linearly with dissolved indole concentration. Next, in order to understand the effects of inter-device variability, three devices per concentration value were independently evaluated. The results of this analysis, which show that inter-device variability does not have a major effect on the mean gray value intensity, are shown in **Figure 3C**. Device exposure to indole analytical standards allowed for the construction of a linear regression model to calculate dissolved indole concentration from a mean gray value intensity output (**Supplementary Figure S6**). Importantly, these experiments also confirmed the feasibility of this novel assay methodology.

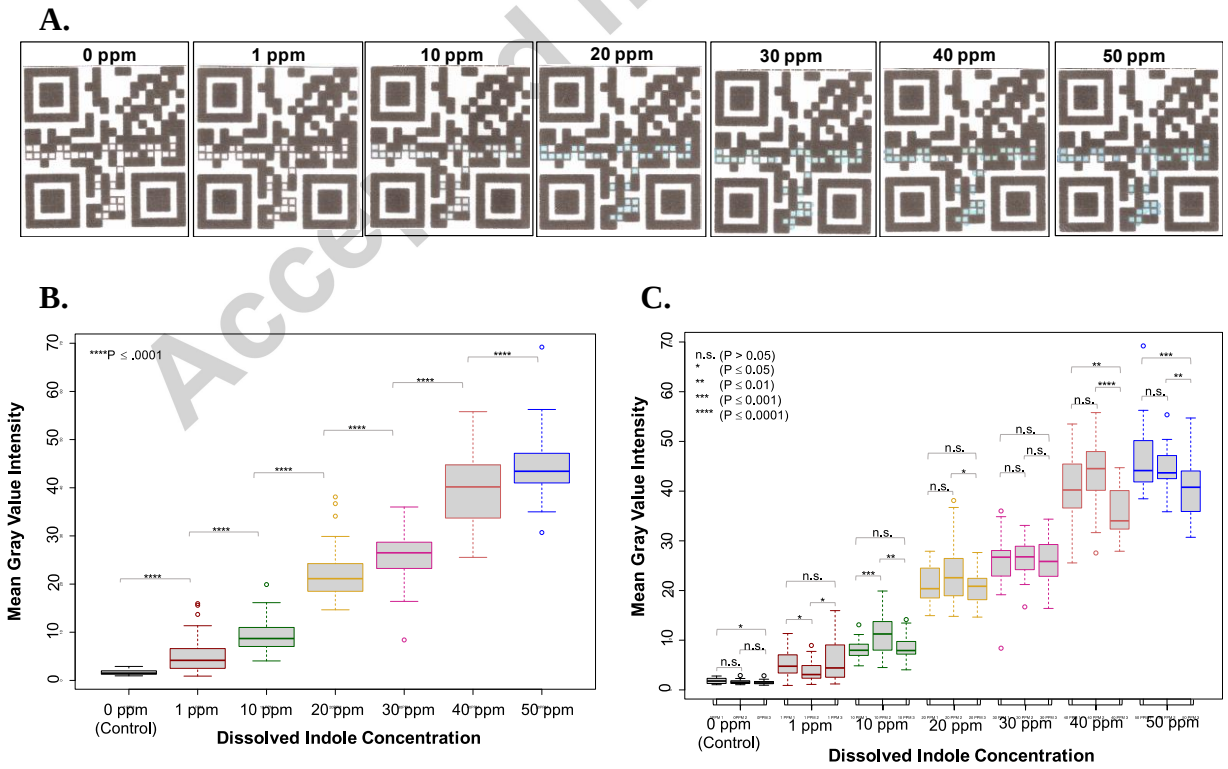

Figure 3. (A) Example images of QR paper sensors post-exposure to indole standard solutions. Solid indole was dissolved in sterile TSB to generate solutions with the following concentrations: 1 ppm, 10 ppm, 20 ppm, 30 ppm, 40 ppm, and 50 ppm. Three devices per concentration value were evaluated. A visible color change was observed at 10ppm. Image processing reveled statistically significant difference in mean gray value intensity between 1 ppm and 0 ppm. **(B)** Box-and-whisker plot demonstrating the linear relationship between dissolved indole concentration and mean gray value intensity. The results for each concentration value represent the data from three devices, equaling a total of 90 unique assay regions. **(C)** Box-and-whisker plot demonstrating the relative reproducibility between devices. For each concentration value, the results for all three exposed devices (30 assay regions each) are independently displayed.

Assay exposure to bacterial culture headspace.

Next, the feasibility and clinical utility associated with employing this assay to detect indole production in *E. coli in vitro* was evaluated. Specifically, indole production was measured in three strains of *E. coli:* 1) *E. coli* K12 (clinical isolate), 2) *E. coli* ATCC 25922 (reference isolate), and 3) *E. coli* 43890 (reference isolate). Three strains of *E. coli* were evaluated in order to affirm that relatively similar quantities of indole within a detectable range are produced by *E. coli* intraspecies. *Pseudomonas aeruginosa* ATCC 27853, a non-indole producing bacteria, was also evaluated as a negative control. Following an overnight pre-culture step, approximately 40 CFU/mL were inoculated into sterile Tryptic Soy Broth (TSB). This low inoculation dose was intentionally chosen to mimic the low cell concentration in patients with sepsis [38, 39]. Further, TSB was intentionally selected as the culture media, as it is most similar to the proprietary media found in blood culture bottles [40]. In order to diagnose sepsis, a blood culture is first required to affirm the presence of a pathogen in the bloodstream, but provides no species-level information. Given that the average time to blood culture positivity is approximately twelve hours [30], time points were selected to assist in *E. coli* species identification either prior to blood culture positivity (3 h, 6 h, 9 h), or at worst, at the time of culture positivity (12 h).

No visible change in color was observed in any of the devices exposed to *E. coli* culture supernatant at 3 h, 6 h, and 9 h. This was true for all three *E. coli* strains evaluated. That said, at 12 h a significant shift in color intensity and pigmentation was observed in all three *E. coli* strain

samples. No significant change was observed in the *P. aeruginosa* or the sterile control samples. The results of these observations are shown in **Figure 4A**. Remarkably, this suggests that indole production in an *E. coli* positive blood culture could be identified at or near the time of blood culture positivity. By employing the linear regression model obtained above, the dissolved indole concentration could be calculated from the obtained mean gray value intensity output. The mean dissolved indole concentration at 12 h for all three *E. coli* strains in combination was 27.0 ± 3.1 ppm. More specifically, the dissolved indole concentration at 12 h was 23.6 ppm for *E. coli* ATCC 43890, 27.8 ppm for *E. coli* K12, and 29.6 ppm for *E. coli* ATCC 25922 (**Figure 4B**). Given this result, a "positive scan" would register approximately within this concentration range for this specific application. The cell concentrations at each of these time points are detailed in

Supplementary Table S7.

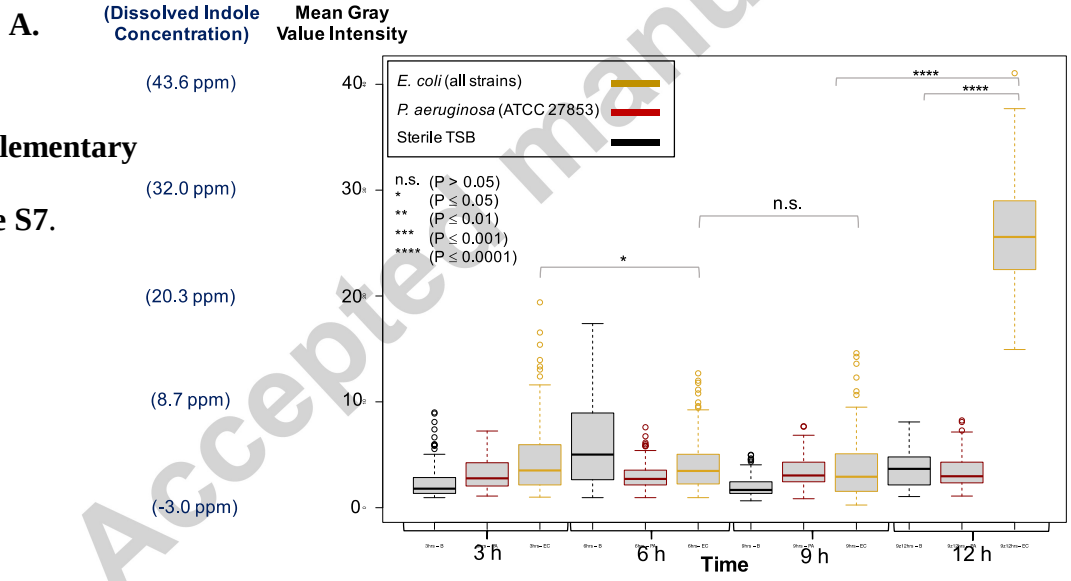

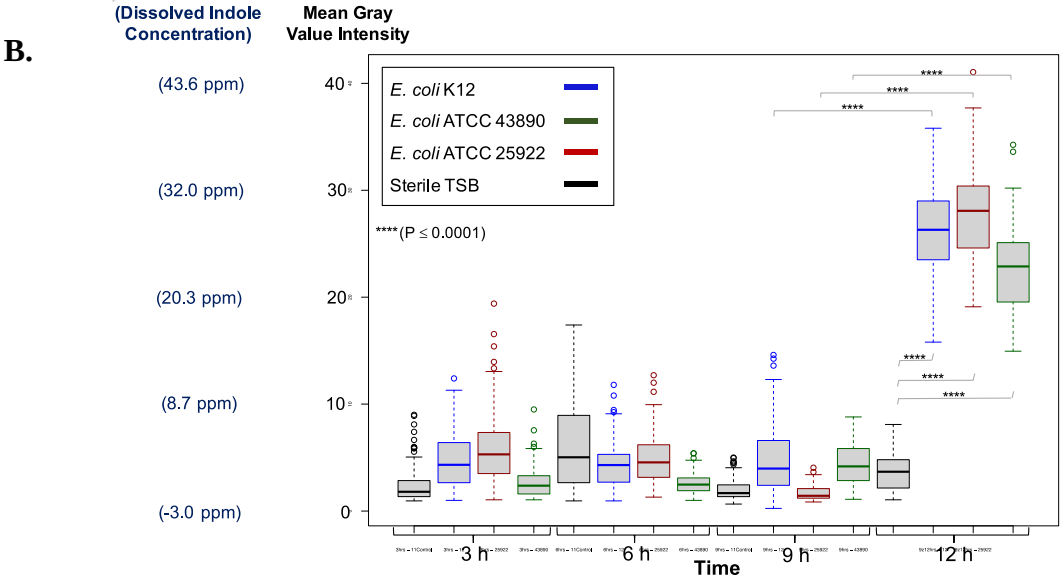

Figure 4. (A) Box-and-whisker plot showing significant increase in mean gray value intensity at 12 h for all three *E. coli* strains in combination. Compiled *E. coli* data at each time point includes 270 data points from a total of 270 assay regions. *P. aeruginosa* results represent the compilation of intensity data from three unique devices at each time point (90 unique assay regions per strain per time point). **(B)** Box-and-whisker plots showing significant increase in mean gray value intensity at 12 h for all three *E. coli* strains independently. The results for each *E. coli* strain represent the compilation of intensity data from three unique devices at each time point (90 unique assay regions per strain per time point).

Quantification of indole production in *E. coli* with HS-SPME GCxGC-TOFMS.

To further assess the performance of the assay, the indole concentration in *E. coli* culture supernatant was quantified using routine headspace solid-phase microextraction (HS-SPME) approach coupled to comprehensive two-dimensional gas chromatography time-of-flight mass spectrometry (GC×GC-TOFMS). It is important to note that the multidimensional chromatography system was not fully exploited due the nature of this targeted application.

The mean chromatogram area for the 12 h time-point *E. coli* samples ranged from 8.28E6 (*E. coli* ATCC 25922) to 1.15E7 (*E. coli* ATCC 43890). In order to determine the dissolved indole concentration from raw chromatogram area values, a calibration curve was built by analyzing indole standards at known concentrations (ranging from 2 to 40 ppm, **Supplementary Figure S8**) and evaluating the corresponding chromatographic area. By employing the obtained linear regression model, dissolved indole concentrations were extrapolated to equal 28.2 ± 2.7 ppm for

E. coli ATCC 25922, 30.5 ± 7.8 ppm for *E. coli* K12, and 38.2 ± 2.8 ppm for *E. coli* ATCC 43890. Further, the mean dissolved indole concentration at 12 h for all three *E. coli* strains in combination was 32.3 ± 5.2 ppm. These dissolved indole concentrations are remarkably similar to those obtained by the QR code paper microfluidic assay, further suggesting that the paper assay is both quantitative and accurate. That said, it is important to emphasize that the paper microfluidic assay is not intended to replace GC×GC-TOFMS. Rather, GC×GC-TOFMS was employed to demonstrate a sufficient correlation between the results obtained by these two methods. Also, due to unavoidable differences between the experimental setup for device exposure and the HS-SPME sampling method, the volatile indole concentration in the sample headspace could be slightly varied.

At the 9 h time point, dissolved indole concentrations were calculated to be 3.5 ± 2.2 ppm for *E. coli* ATCC 25922, 3.4 ± 2.6 ppm for *E. coli* K12, and 3.1 ± 2.4 ppm for *E. coli* ATCC 43890. Although these values are significantly lower in magnitude than the 12 h time point values, they were statistically sufficient to detect the presence of indole. Indole was not detected at significant levels prior to 9 h. Due to the high sensitivity and cost associated with this analytical instrumentation, it is not surprising that indole was detected at an earlier than observed in the paper device. Although this could be a beneficial methodology to employ in state-of-the-art clinical microbiology facilities to assist in *E. coli* species identification, this type of instrumentation is not feasible to employ in lower income countries, or facilities that do not have the funding to support this type of instrumentation.

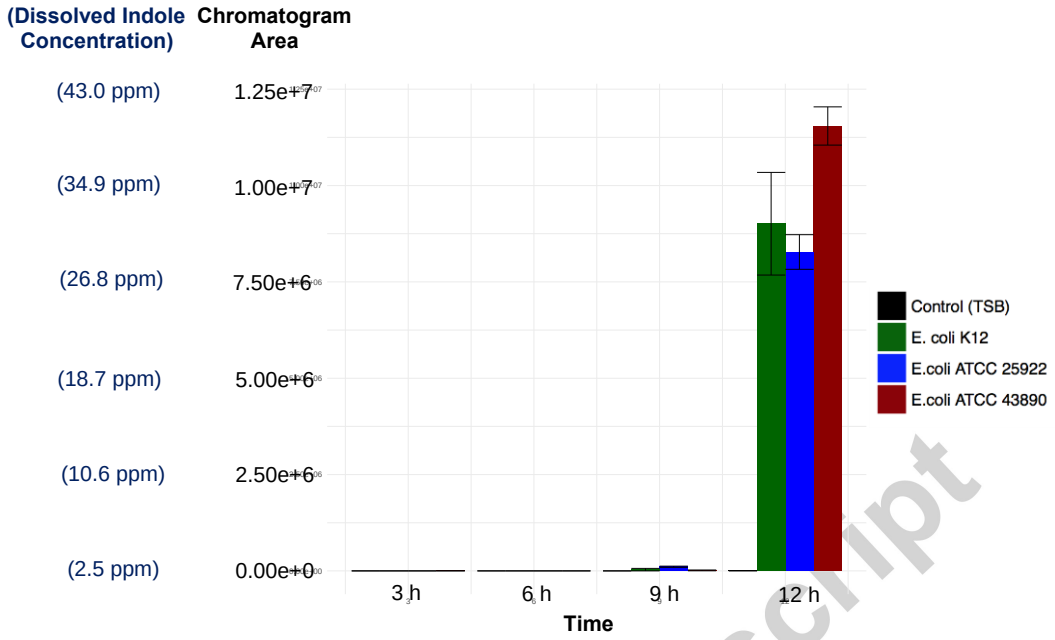

Figure 5. Chromatogram area and extrapolated dissolved indole concentration of *E. coli* strains from HS-SPME GCxGC-ToFMS analysis. 12 h data are the average of three samples with standard error of the mean displayed. 9 h data are the average of 2 samples.

Discussion

In this report we discuss the development of an integrated QR code paper microfluidic colorimetric assay for use in low-resource environments. We demonstrate this platform's functionality within the context of a specific and novel application: volatile indole detection to assist in the rapid identification of *E. coli* in bloodstream infections. To the best of our knowledge only one prior study has demonstrated the feasibility of employing *p*-dimethylaminocinnamaldehyde (DMACA) for the detection of indole in the gas-phase. Specifically, Crunaire, et al. demonstrated that the use of nanoporous matrices doped with DMACA could discriminate *E. coli* from non-indole producing bacteria on solid agar prior to colonies becoming visible to the naked eye [41]. That said, no prior work has demonstrated the use of a paper substrate saturated with DMACA to detect indole from the headspace of a liquid culture. Not only did we demonstrate the ability to detect indole in the headspace of *E. coli*

culture using a paper device, we also demonstrated that this assay can be quantitative, given the observed linear relationship between dissolved indole concentration and mean gray value intensity. Although knowledge of bacterial concentration is not relevant in the diagnosis and treatment of bloodstream infections, this type of information could be useful in employing the assay for other diagnostic applications. For example, in the diagnosis of urinary tract infections (UTIs), bacterial load is a key variable affecting the diagnosis and treatment regimen [42].

Conclusions

This study is the first to demonstrate the use of paper-based QR device as an effective colorimetric diagnostic assay. Aside from being a rapid diagnostic platform which can be printed with well-defined arrays, this system enables the centralized collection of epidemiological data to inform clinicians and policy makers of statistics surrounding patient populations of interest. Moving forward, we envision that the proposed platform can be extended to other colorimetric assays for broader use in low-resource environments.

Acknowledgements

The authors would like to acknowledge Dr. Joseph D. Schwartzman and the Clinical Microbiology team at Dartmouth Hitchcock Memorial Hospital in Lebanon, NH for sharing their expertise on the diagnostic workflow for bloodstream infections. Harrison Hall would also like to thank and acknowledge the support of the Ralph and Marjorie Crump Innovation Fellowship for the support of this research. Partial financial support was provided by National Science Foundation grants (ECCS 1128677, 1309686, 1509369, PI: Zhang).

Author Contributions

Alison Burklund conducted all experiments. Harrison K. Hall designed the QR code algorithm and all associated software. Flavio A. Franchina provided guidance and assisted with GCxGC-TOFMS methodology and experiments. Dr. Jane E. Hill provided advice on candidate volatile biomarkers for infectious disease, and use of her lab space and analytical equipment. Dr. John X.J. Zhang and Harrison K. Hall perceived the concept of QR code based microfluidic assays, and Dr. Zhang provided expertise on device fabrication and design. Alison Burklund wrote the manuscript with contributions from Harrison K. Hall. All coauthors reviewed and approved the manuscript.

Competing financial interests

The authors declare no competing interests or conflict of interests.

References

1. Yager P., *et al*. Microfluidic diagnostic technologies for global public health. *Nature* **442**, 412– 418 (2006).
2. King, E.J. & Garner, R.J. The Colorimetric Determination of Glucose. *Journal of Clinical Pathology* **1**, 30–33 (1947).
3. Bartos, J. & Pesez, M. Colorimetric and flourimetric determination of aldehydes and ketones. *Pure & Applied Chemistry* **51**,1803–1814 (1979).
4. Sapan, C.V., Lundblad, R.L. & Price, N.C. Colorimetric protein assay techniques. *Biotechnology & Applied Biochemistry* **29**, 99–108 (1999).

5. Gao, Z., Hou L., Xu, M. & Tang, D. Enhanced Colorimetric Immunoassay Accompanying with Enzyme Cascade Amplification Strategy for Ultrasensitive Detection of Low-Abundance Protein. *Scientific Reports* **4**, 3966 (2014).

6. Zhou, W.H., Zhu, C.L., Lu, C.H., Guo, X., Chen, F., Yang H.H., & Wang X. Amplified detection of protein cancer biomarkers using DNAzyme functionalized nanoprobes. *Chemical Communications* **0**, 6845– 7 (2009).

7. Hosokawa, K., Fujiiand, T. & Endo, I. Handling of Picoliter Liquid Samples in a Poly(dimethylsiloxane)-Based Microfluidic Device. *Analytical Chemistry* **71**, 4781– 4785 (1999).

8. Lee, D.S., Jeon, B. G., Ihm, C., Park, J.K. & Jung M. Y. A simple and smart telemedicine device for developing regions: a pocket-sized colorimetric reader. *Lab on a Chip* **11**, 120–6 (2011).

9. Haeberle, S., Mark, D., Von Stetten, F., & Zengerle, R. Microfluidic platforms for lab-on-a-chip applications. *Microsystems and Nanotechnology* **9783642182**, 853–895 (2007).

10. Carrilho, E., Martinez, A.W. & Whitesides, G.M. Understanding Wax Printing: A Simple Micropatterning Process for Paper-Bases Microfluidics. *Anal. Chem.* **81**, 7091-7095, (2009).

11. Osborn, J.L., Lutz, B., Fu, E., Kauffman, P., Stevens, D.Y. & Yager, P. Microfluidics without pumps: reinventing the T-sensor and H-filter in paper networks. *Lab on a Chip*, **10**, 2659–2665 (2010).

12. Washburn, E.W. The Dynamics of Capillary Flow. *The Physical Review* **17**, 273 (1921).

13. Falas, T. & Kashani, H. Proceedings - Fifth Annual IEEE International Conference on Pervasive Computing and Communications Workshops. *PerCom Workshops* **2007**, 597–600 (2007).

14. ISO. *ISO Standards*, **2000**., 122 (2000).

15. Kwon, H., Park, J., An, Y., Sim, J. & Park, S. A smartphone metabolomics platform and its application to the assessment of cisplastin-induced kidney toxicity. *Analytica Chimica Acta* **845**, 15–22 (2014).

16. Thom, N.K., Lewis, G.G., Yeung, K., & Phillips, S. T. (2014). Quantitative Fluorescence Assays Using a Self-Powered Paper-Based Microfluidic Device and a Camera-Equipped Cellular Phone. *RSC Advances* **4**, 1334–1340 (2014).

17. Fang, X., Wei, S. & Kong, J. Paper-based microfluidics with high resolution, cut on a glass fiber membrane for bioassays. *Lab on a Chip* **14**, 911–5 (2014).

18. Mariella, R. Jr. Sample preparation: the weak link in microfluidics-based biodetection. *Biomedical Microdevices* **10**, 777 (2008).

19. Leber, A.L. Clinical Microbiology Procedures Handbook, Fourth Edition. *American Society for Microbiology.* (2016).

20. Mahon, C.R., Lehman, D.C. & Manuselis, G. Textbook of Diagnostic Microbiology: Fifth Edition. *Elsevier.* (2014).

21. Lever A., & Mackenzie, I. Sepsis: definition, epidemiology, and diagnosis. *British Medical Journal* **335,** 879-883 (2007).

22. Gracias, K.S. & McKillip, J.L. A review of conventional detection and enumeration methods for pathogenic bacteria in food. *Canadian Journal of Microbiology* **50,** 883-890 (2004).

23. Li, G. & Young, K.D. Indole production by the trytophanse TnA in *Escherichia coli* is determined by the amount of exogenous tryptophan. *Microbiology* **159,** 402-410 (2013).

24. Isenberg, H.D. & Sundheim, L.H. Indole reactions in bacteria. *J. Bacteriol* **75**, 682 – 690 (1958).

25. Turner, J.M. A New Reagent for the Assay of Indole in the Trytophanase Reaction. *Journal of Biochemistry* **78**, 790-792 (1961)**.**

26. Lowrance, B.L., Reich, P. & Traub, W. H. Evaluation of Two Spot Indole Reagents. *Applied Microbiology* **17**, 923-924 (1969).

27. Miller, J.M., & Wright, J.W. Spot Indole Test: Evaluation of Four Reagents. *Journal of Clinical Microbiology* **15**, 589-592 (1982).

28. Mayr, F.B., Yende, S. & Angus, D.C. Epidemiology of severe sepsis. *Virulence* **5,** 4-11 (2014).

29. Lee, J.H. & Lee, J. Indole as an intercellular signal in microbial communities. *FEMS Microbiology Reviews* **34**, 426-444 (2010).

30. Mateos, F. & De Benito, I. Time-to-positivity in patients with *Escherichia coli* bacteremia. *Clinical. Microbiology and. Infection* **13**, 1077-1082 (2007).

31. Murray, P.R. & Masur, H. Current Approaches to the Diagnosis of Bacterial and Fungal Bloodstream Infections for the ICU. *Critical Care Medicine* **40**, 3277-3282 (2014).

32. Liesenfeld, O., Lehman, L., Hunfeld, K.P. & Kost, G. Molecular Diagnosis of Sepsis: New Aspects and Recent Developments. European Journal of Microbiology and Immunology **4**, 1-25 (2014).

33. Beekmann, S. E., Diekema, D.J., Chapin, K.C. & Doern, G.V. Effects of Rapid Detection of Bloodstream Infections on Length of Hospitalization and Hospital Charges. *Journal of Clinical. Microbiology* **41**, 3119–3125 (2003).

34. Leibovici, L., Shraga, I., Drucker, M., Konigsberger, H., Samra, Z. & Pitlik, S.D. The benefit of appropriate empirical antibiotic treatment in patients with bloodstream infection. *Journal of Internal Medicine* **244**, 379–386 (1998).

35. Tranchida, P.Q., Franchina, F.A., Dugo, P. & Mondello, L. Comprehensive two-dimensional gas chromatography-mass spectrometry: recent evolution and current trends. *Mass Spectrometry Reviews* **35,** 524–534 (2016).

36. Owen, S. ZXing. https://github.com/zxing/zxing

37. Bean, H.D., Dimandja, J.M.D. & Hill, J.E. Bacterial volatile discovery using solid phase microextraction and comprehensive two-dimensional gas chromatography–time-of-flight mass spectrometry. *Journal of Chromatography B, Analytical Technologies in the Biomedical & Life Sciences* **901**, 41–46 (2012).

38. Kreger, B.E., Craven, D.E., Carling, P.C. & McCabe W.R. Gram-negative bacteremia. III. Reassessment of etiology, epidemiology and ecology in 612 patients. *American Journal of Medicine* **68**, 332-343 (1980).

39. Yagupsky, P. & Nolte, F.S. Quantitative Aspects of Septicemia. *Clinical Microbiology Reviews* **3**, 269-279 (1990).

40. Hall, M.M., Ilstrup, D.M. & Washington II, J.A. Comparison of Three Blood Culture Media with *Tryptic Soy Broth. Journal of Clinical Microbiology* **8**, 299-301 (1978).

41. Crunaire, S., *et al*. Discriminating Bacteria with Optical Sensors Based on Functionalized Nanoporous Xerogels. *Chemosensors.* **2**, 171-181 (2014).

42. Wilson, M.L. & Gaido, L. Laboratory diagnosis of urinary tract infections in adult patients. *Clinical Infectious Diseases* **38**, 1150-1158 (2004).

Highlights

- Volatile indole can be detected on a paper substrate with a colorimetric reagent
- Colorimetric signal correlates linearly with volatile indole concentration
- Indole can be colorimetrically detected in the headspace of *E. coli* culture
- Benchmarking with GCxGC-TOFMS showed that paper sensor measurements were accurate
- Digital QR code paper-based microfluidic sensors are feasible diagnostic platforms